

PHASE RETRIEVAL IN 3D X-RAY MAGNIFIED PHASE NANO CT: IMAGING BONE TISSUE AT THE NANOSCALE

Boliang Yu⁽¹⁾, Loriane Weber^(1,2), Alexandra Pacureanu⁽²⁾, Max Langer^(1,2), Cecile Olivier^(1,2), Peter Cloetens⁽²⁾, Françoise Peyrin^(1,2)

1. Creatis, Inserm U1206, CNRS 5220, INSA Lyon, UCBL, 69621 Villeurbanne, France

2. ESRF, 38043 Grenoble, France

ABSTRACT

X-ray phase computed tomography (CT) offers higher sensitivity than conventional X-ray CT. A new phase-CT instrument producing a nano-focused beam has been developed at the ESRF (European Synchrotron Radiation Facility) for nano-imaging. In order to obtain final images, a suited phase retrieval algorithm is necessary, which is attracting broader interest recently. In this paper, we explicit the 3D phase CT image reconstruction problem, including the stage of phase retrieval prior to 3D CT reconstruction. The phase retrieval problem is solved by extending the single distance Paganin method to multi-distance acquisitions, followed by an iterative non-linear conjugate gradient descent optimization method. The method is evaluated on bone tissue samples imaged at voxel sizes of 120 nm. The results obtained from acquisition at 1 and 4 distances, with and without the iterative refinement are compared. The results show that this method yields improved images compared to other methods.

Index Terms— phase contrast, phase retrieval, X-ray nano-tomography, bone imaging

1. INTRODUCTION

With the development of third-generation synchrotron radiation sources, X-ray phase imaging has made great progress for the observation of biological tissues and materials. The advantage of X-ray phase imaging is that it offers higher sensitivity than attenuation-based imaging [1]. Phase CT is based on X-ray phase contrast, where first phase maps are retrieved at each projection angle, and then used to reconstruct the real part of the refractive index (phase shift) in 3D, instead of the imaginary part (attenuation) in standard CT [2]. Actually, the recorded intensity images contain contrast both from attenuation and phase shift induced by the sample, but these two quantities are non-linearly entangled in the intensity and therefore

cannot be accessed directly. It is thus necessary to estimate the phase shift from the recorded intensity. This step is called “phase retrieval” and is a non-linear inverse problem.

Among the different experimental techniques allowing phase CT, we study the one based on free-space propagation, which consists in placing the detector at several propagation distances from the object. Phase micro-CT has already provided successful images of small animals or biological samples at micrometric scale [3], [4], [5].

In this work, we used a new 3D X-ray phase synchrotron nano-CT setup developed at beamline ID16A of the ESRF, which targets an isotropic pixel size up to 20 nm [6]. The incoming parallel X-ray beam is monochromatized and focused by curved reflective (Kirkpatrick-Baez) optics (Figure 1). The goal is to image bone ultrastructure in the context of the prediction of bone failure in diseases such as osteoporosis. Bone has a complex hierarchical structure and its strength relies on all scales, from the organ level to the sub-cellular scale [7].

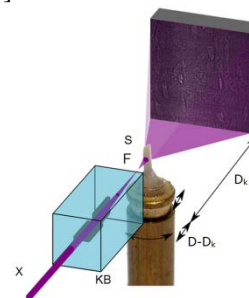


Figure 1: Scheme of experimental setup of magnified phase nano-CT setup. X denotes the incoming X-ray beam, F the focal spot of the beam, S the sample, D the detector [6]

The direct image formation problem can be modeled by the Fresnel diffraction, where the recorded intensity is expressed as the squared magnitude of the Fresnel transform of the transmittance function of the sample. It is difficult to directly use this model for phase retrieval because of the non-linear relationship.

To address this problem, two classical approaches to linearize the problem have been developed. On one hand, the transport of intensity equation (TIE) is based on a first order Taylor expansion of the intensity with respect to the distance between object and detector, and is only valid within a range of small distances [8]. On the other hand, the contrast transfer function (CTF) is based on a first order Taylor expansion of the intensity with respect to the wave, and is valid for weak absorption and slowly varying phase [9]. Both approaches are linear and can be inverted by Fourier filtering. A mixed method has also been proposed, which asymptotically combines the CTF and TIE extending validity to both long distances and absorbing (but slowly varying) objects [10].

A convenient formula that can be used from a single phase contrast image was derived by Paganin, based on the TIE model under the assumption that the object is homogeneous [11]. It is essentially a Fourier low-pass filter which can be applied directly on the recorded images.

Here, we develop a method which extends Paganin's single distance method to multiple distance acquisitions. This method is applied to bone tissue samples imaged at isotropic voxel sizes of 120 nm. We show that the quality of the reconstruction is improved in terms of spatial resolution and signal-to-noise ratio when several images recorded at different distances are used.

2. DIRECT PROBLEM

The interaction between X-rays and matter in a 3D object can be modeled by its refractive index distribution [10],

$$n(x, y, z) = 1 - \delta_n(x, y, z) + i\beta(x, y, z) \quad (1)$$

where δ_n is the refractive index decrement, β , the absorption coefficient and (x, y, z) denotes the 3D spatial coordinates.

Let us assume a coherent X-ray beam of wavelength λ , propagating in the z direction through the object. The transmittance function $T(\mathbf{x})$, where $\mathbf{x} = (x, y)$ are the coordinates in the plane perpendicular to z , describes the wave at the output of the object:

$$\begin{aligned} T(\mathbf{x}) &= a(\mathbf{x}) \exp[i\varphi(\mathbf{x})] = \exp[-B(\mathbf{x}) + i\varphi(\mathbf{x})] \\ B(\mathbf{x}) &= (2\pi/\lambda) \int \beta(x, y, z) dz \\ \varphi(\mathbf{x}) &= -(2\pi/\lambda) \int \delta_n(x, y, z) dz \end{aligned} \quad (2)$$

where, $B(\mathbf{x})$ the attenuation caused by the object, $a(\mathbf{x})$ the amplitude and $\varphi(\mathbf{x})$ the phase shift of the wave.

If the beam propagates in free space over a distance D_k , where k is the distance index, the recorded intensity can be modeled as the squared modulus of the Fresnel Transform:

$$\begin{aligned} I_{D_k}(\mathbf{x}) &= |T(\mathbf{x}) * P_{D_k}(\mathbf{x})|^2 \\ P_{D_k}(\mathbf{x}) &= \frac{1}{i\lambda D_k} \exp\left(i \frac{\pi}{\lambda D_k} |\mathbf{x}|^2\right) \end{aligned} \quad (3)$$

The Fourier transform of the intensity $I_{D_k}(\mathbf{x})$, denoted $\tilde{I}_{D_k}(\mathbf{f})$ can be written directly as [10]:

$$\tilde{I}_{D_k}(\mathbf{f}) = \int T\left(\mathbf{x} - \frac{\lambda D_k \mathbf{f}}{2}\right) T^*\left(\mathbf{x} + \frac{\lambda D_k \mathbf{f}}{2}\right) \exp(-i2\pi \mathbf{x} \cdot \mathbf{f}) d\mathbf{x} \quad (4)$$

where $\mathbf{f} = (f_x, f_y)$ are the 2D coordinates conjugate to \mathbf{x} in Fourier space.

3. PHASE RETRIEVAL

The Paganin's method estimates the phase shift from an intensity image recorded at D_k by exploiting the TIE model and assuming that the object is homogeneous. A homogeneous object has a constant δ_n/β ratio (real-to-imaginary part of the refractive index). The composition is assumedly known, and this ratio is given as a parameter to the algorithm. For a given chemical composition, it can be calculated e.g. using the X-ray optics software XOP [12]. Paganin's method gives the following inversion formula:

$$\varphi(\mathbf{x}) = \frac{1}{2} \cdot \frac{\delta_n}{\beta} \cdot \ln \left(\mathcal{F}^{-1} \left\{ \frac{\mathcal{F}(I_{D_k}/I_{Inc})(\mathbf{f})}{1 + \lambda D_k \pi \frac{\delta_n}{\beta} \|\mathbf{f}\|^2} \right\}(\mathbf{x}) \right) \quad (5)$$

where $I_{Inc}(\mathbf{x})$ is the incoming intensity and \mathcal{F} (resp. \mathcal{F}^{-1}) denotes the direct (resp. inverse) Fourier Transform.

We introduce the following notations to make the formula more concise:

$$\begin{aligned} \tilde{I}_{norm,k}(\mathbf{f}) &= \mathcal{F}\left(\frac{I_{D_k}}{I_0}\right)(\mathbf{f}), \quad \tilde{H}_k(\mathbf{f}) = 1 + \frac{D_k \delta_n \lambda \pi}{\beta} \|\mathbf{f}\|^2 \\ \tilde{A}(\mathbf{f}) &= \mathcal{F} \left\{ \exp\left(\frac{2\beta}{\delta_n} \varphi(\mathbf{x})\right) \right\}(\mathbf{f}) \end{aligned} \quad (6)$$

According to (5) and (6), we have:

$$\tilde{I}_{norm,k}(\mathbf{f}) = \tilde{A}(\mathbf{f}) \tilde{H}_k(\mathbf{f}) \quad (7)$$

Thus the Paganin's method can be equivalently seen as performing an inverse filter to retrieve $A(\mathbf{f})$ from $\tilde{I}_{norm,k}(\mathbf{f})$.

When different distances D_k for $k = 1, \dots, K$ are considered, the problem can be seen as a linear least squares minimization. If including Tikhonov regularization, the phase shift can be estimated as:

$$\hat{\varphi}(\mathbf{x}) = \frac{1}{2} \cdot \frac{\delta_n}{\beta} \cdot \ln \left(\mathcal{F}^{-1} \left\{ \frac{\frac{1}{K} \sum_{k=1}^K \tilde{H}_k(\mathbf{f}) \cdot \tilde{I}_{norm,k}(\mathbf{f})}{\left(\frac{1}{K} \sum_{k=1}^K \tilde{H}_k(\mathbf{f})^2\right) + \alpha} \right\}(\mathbf{x}) \right) \quad (8)$$

where α is an arbitrary regularization parameter.

To refine the solution, an iterative non-linear conjugate gradient method is applied [6]. The solution given by equation (8) is used as initialization.

4. DATA ACQUISITION AND RECONSTRUCTION

All data were acquired at beamline ID16A, ESRF, Grenoble, France, a long beamline (185m from the source) providing a highly coherent, high-brilliance beam at specific energies (17 keV or 33.6 keV) [13]. Transverse cross-sections were cut from mid-diaphysis in femurs from women (50-95 years old). Then, small cortical bone samples ($0.4 \times 0.4 \times 3$ mm³) were prepared using a high precision saw.

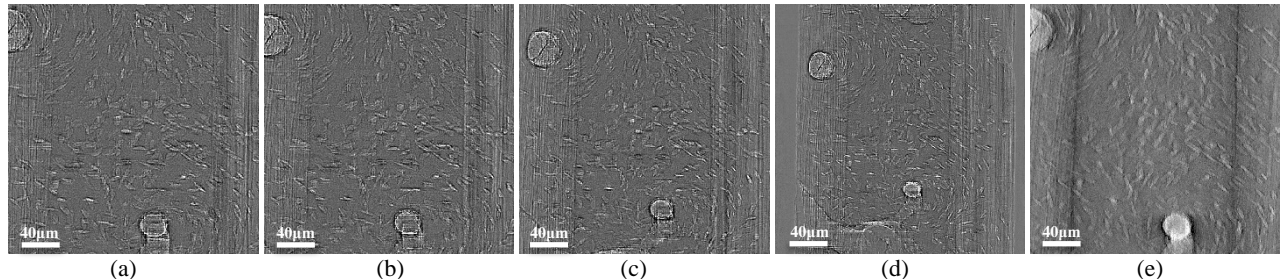


Figure 2: Illustration of the recorded images and retrieved phase map. Raw projections at 4 focus-to-sample distances (a) 50.53 mm, (b) 52.70 mm, (c) 61.37 mm and (d) 79.37 mm; (e) a retrieved phase map

Each sample was put under vacuum on a sample stage and rotated over a range of 180° to obtain a tomographic scan of 2000 projections. The process was repeated at 4 different sample-to-detector distances. The X-ray beam propagated to the detector after traversing the sample is converted into visible light by a scintillator, then recorded by a FReLoN (Fast Readout Low Noise) $(2048)^2$ CCD [6].

In practice, the position of the detector is fixed while the sample is moved downstream of the focus [14]. The recorded images at the different distances have slightly different magnifications (Figure 2). If D_k (resp. $D - D_k$) is the sample to detector (resp. focus) distance, the magnification is $M = D/(D - D_k)$ (Figure 1). The highest magnification corresponds to the first distance.

Data acquisition was performed for pixels sizes of 120 and 30 nm. Acquisition time for a complete dataset (i.e. with 4 propagation distances) was approximately 4 hours. For each sample, the processing includes resampling the remaining images to the highest resolution, registration of images at different distances, phase retrieval, and CT reconstruction performed by a standard filtered back-projection (FBP) algorithm.

Different methods were tested for phase retrieval: simple and extended Paganin approach from one distance to four distances, and both with and without iterative refinement. The δ_n/β ratio was set to 645, which corresponds to the theoretical value for bone at 33.6 KeV.

5. RESULTS

Figure 2 illustrates the raw $(2048)^2$ projections of the sample at four distances as well as a retrieved phase map. Among the different methods that were tested, we observed that the reconstruction was improved by using an increasing number of distances with the extended Paganin’s approach. Due to space constraints, we only show the results from 1 and 4 distances for the images at 120 nm. Figure 3 (a), (b), (c) and (d) show reconstructed tomographic slices in the middle of the same sample, with 1 and 4 distances, with and without iterative refinement. The back ellipsoidal structures correspond to osteocyte lacunae (imprint of cells) connected by canaliculi (small channels left by the osteocytes dendrites). For visibility, we display Maximum Intensity

Projections (MIP) on 100 slices which better shows the small channels. The 3D image size is $(2048)^3$ corresponding to a field of view of $245\mu\text{m}$ in each direction. Figure 3 (e), (f), (h), (i) display zooms around one lacuna in the middle slice corresponding to (a), (b), (c) and (d) respectively, and Figure 3 (i) shows profiles through the zoomed regions. If we compare (a) with (c), (b) with (d), it can be seen that the image reconstructed from a single distance is more blurred and the result is improved when using 4 distances. This visual observation is confirmed by looking at the profiles, which show that the background of the reconstructed image using 4 distances has less low frequency noise than that using a single distance, hence it is flatter. Further, comparing (a) and (b), (c) and (d), we can see that the iterative process permits to improve the sharpness at the cost of longer execution time for the conjugate gradient method.

To measure the gain in image quality, we also estimated the spatial resolution around one lacuna. This was performed by fitting the Edge Spread Function with an erf function and estimating the Full Width Half Maximum (FWHM). We also calculated the spatial resolution defined at 10% of the cut of frequency of the Fourier Modulation Transfer Function. Table 1 shows the different results. The extended Paganin’s method for 4 distances and 10 iterations provides the best spatial resolution.

Paganin's method	FWHM	Resolution
1 distance, no iteration	1.39 μm	0.86 μm
1 distance, 10 iterations	0.69 μm	0.43 μm
4 distances, no iteration	1.56 μm	0.97 μm
4 distances, 10 iterations	0.47 μm	0.29 μm

Table 1: FWHM and spatial resolution for different conditions

6. CONCLUSION

We used X-ray phase nano-CT to image bone tissue from data sets of phase contrast projections at different propagation distances. After presenting the phase retrieval problem, we proposed an extension of the Paganin inversion formula to take into account several distances. The method was evaluated on experimental bone data. Our results show that reconstructions are sharper with better contrast when using 4 distances with an iterative refinement.

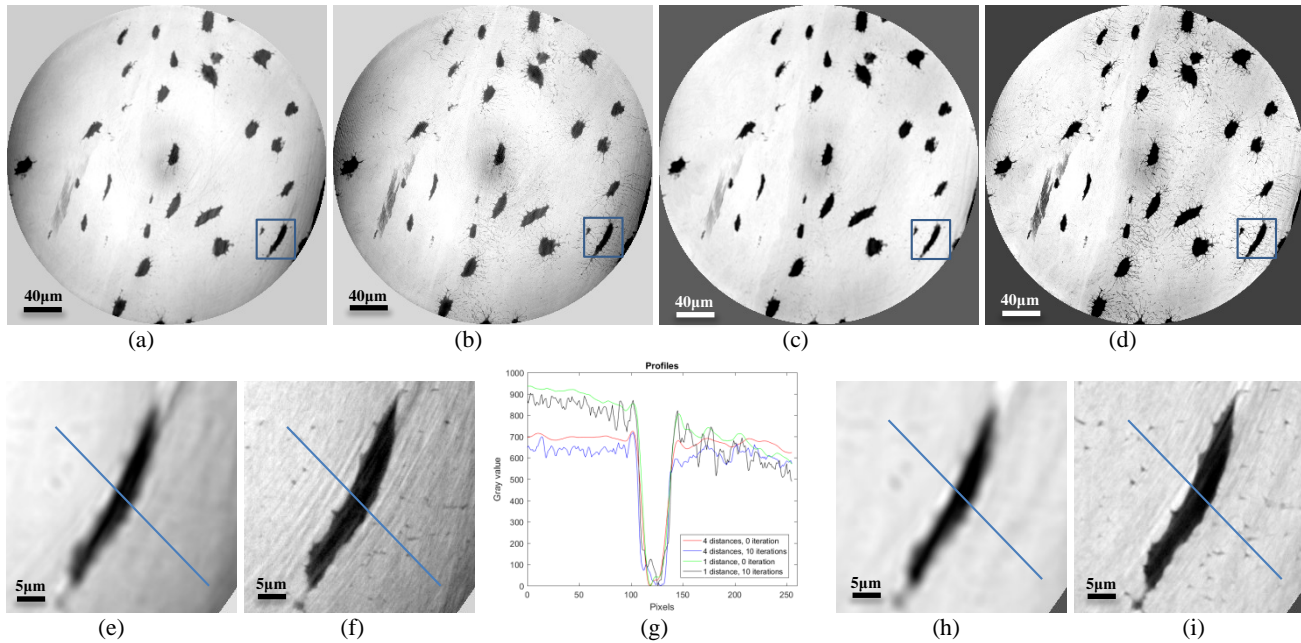


Figure 3: Top: Maximum Intensity Projections (MIP) of reconstructions by single and extended Paganin's method from 1 and 4 distances (a) 1 distance without iteration; (b) 1 distance with 10 iterations; (c) 4 distances without iteration; (d) 4 distances with 10 iterations; Bottom (e), (f), (h) and (i): zooms of the middle slice around one lacuna corresponding to (a), (b), (c) and (d) respectively; (g) profiles across the line marked in the different zoomed regions

The combination of several different propagation distances allows a better coverage of the Fourier domain of the phase projections, thus finally of the object due to the Fourier slice projection. Moreover, the simultaneous usage of four distances has the advantage to average errors due to the inhomogeneity of the beam and to reduce ring artifacts. In future works, this method will be used on data sets at higher spatial resolution to quantify one ultrastructure.

7. ACKNOWLEDGEMENTS

This work was supported by the ANR grant ANR-14-CE35-0030-01 and by the Région Rhône-Alpes. It was also done in the framework of LabEx PRIMES (ANR-11-LABX-006"). We thank the ESRF for support through the LTP MD830.

8. REFERENCES

- [1] A. Momose, "Recent Advances in X-ray Phase Imaging," *Jpn. J. Appl. Phys.*, vol. 44, no. 9A, pp. 6355–6367, Sep. 2005.
- [2] A. Momose, "Phase-sensitive imaging and phase tomography using X-ray interferometers," *Opt. Express*, vol. 11, no. 19, p. 2303, Sep. 2003.
- [3] R. Boistel et al., "How minute sooglossid frogs hear without a middle ear," *Proc. Natl. Acad. Sci.*, vol. 110, no. 38, pp. 15360–15364, Sep. 2013.
- [4] M. Marinescu et al., "Synchrotron Radiation X-Ray Phase Micro-computed Tomography as a New Method to Detect Iron Oxide Nanoparticles in the Brain," *Mol. Imaging Biol.*, vol. 15, no. 5, pp. 552–559, Oct. 2013.
- [5] M. Langer, P. Cloetens, and F. Peyrin, "Regularization of Phase Retrieval With Phase-Attenuation Duality Prior for 3-D Holotomography," *IEEE Trans. Image Process.*, vol. 19, no. 9, pp. 2428–2436, Sep. 2010.
- [6] M. Langer, A. Pacureanu, H. Suhonen, Q. Grimal, P. Cloetens, and F. Peyrin, "X-Ray Phase Nanotomography Resolves the 3D Human Bone Ultrastructure," *PLoS ONE*, vol. 7, no. 8, p. e35691, Aug. 2012.
- [7] J. D. Currey, *Bones: structure and mechanics*, 2nd print. and 1. pbk. print. Princeton: Princeton Univ. Press, 2006.
- [8] M. R. Teague, "Irradiance moments: their propagation and use for unique retrieval of phase," *J. Opt. Soc. Am.*, vol. 72, no. 9, p. 1199, Sep. 1982.
- [9] P. Cloetens et al., "Holotomography: Quantitative phase tomography with micrometer resolution using hard synchrotron radiation x rays," *Appl. Phys. Lett.*, vol. 75, no. 19, p. 2912, 1999.
- [10] J. P. Guigay, M. Langer, R. Boistel, and P. Cloetens, "Mixed transfer function and transport of intensity approach for phase retrieval in the Fresnel region," *Opt. Lett.*, vol. 32, no. 12, p. 1617, Jun. 2007.
- [11] D. Paganin, S. C. Mayo, T. E. Gureyev, P. R. Miller, and S. W. Wilkins, "Simultaneous phase and amplitude extraction from a single defocused image of a homogeneous object," *J. Microsc.*, vol. 206, no. 1, pp. 33–40, Apr. 2002.
- [12] M. S. del Rio and R. J. Dejus, "Status of XOP: an x-ray optics software toolkit," in *Optical Science and Technology, the SPIE 49th Annual Meeting*, 2004, pp. 171–174.
- [13] P. Cloetens et al., "Biomedical applications of X-ray nano-imaging," in *Medical Applications of Synchrotron Radiation MASR 2015*, Villard de Lans, France, 2015.
- [14] M. Langer, Y. Liu, F. Tortelli, P. Cloetens, R. Cancedda, and F. Peyrin, "Regularized phase tomography enables study of mineralized and unmineralized tissue in porous bone scaffold: regularized phase tomography," *J. Microsc.*, vol. 238, no. 3, pp. 230–239, Jan. 2010.